Progress In Electromagnetics Research B, Vol. 16, 389–406, 2009

A NOVEL WIDE-BAND MICROSTRIP YAGI-UDA ARRAY ANTENNA FOR WLAN APPLICATIONS

M. Bemani and S. Nikmehr

Faculty of Electrical Engineering
University of Tabriz
Tabriz, Iran

Abstract—This paper presents a design of Wide-Band Microstrip Yagi-Uda antenna with high gain and high front to back (F/B) ratio. Numerical and measured results of our design show more than 18 dB front to back ratio at 5.5 GHz and no backward radiation at 5.2 GHz. An impedance bandwidth of 22.05% was achieved around 5.5 GHz. The antenna gain (10–12.4 dBi) can be varied to be suitable for various applications. Measured return loss and radiation pattern of this antenna is presented to validate the results of simulations by two methods. The first method based on finite element method (FEM) and the second one based on finite integral technique (FIT) were used to analyze antenna structure, and subsequently the Genetic Algorithm (GA) was applied by using HFSS simulator to obtain the optimized parameters. In order to find the best design method for this antenna, the effect of distance between the parasitic elements of proposed antenna was studied. Finally two microstrip Yagi-Uda array antennas were combined to increase the gain of antenna. To demonstrate the major benefits, a comparison of our initial and final designs of Yagi-Uda antenna is provided.

1. INTRODUCTION

These days numerous research activities are being pursued on the subject of wireless communications, which use the microwave or millimeter band [1, 2]. We have witnessed a tremendous growth of wireless communication links in recent years. Most wireless networks use omni-directional antennas [3]. However, in some applications we need directional antennas such as Log Periodic and

Corresponding author: M. Bemani (bemani63@gmail.com).

Yagi-Uda antennas [4–7]. These types of antennas find their use in many applications such as industrial, medical, radar and wireless communications. The microstrip Yagi-Uda array consists of a driven microstrip antenna along with several parasitic microstrip antennas which are arranged on the same substrate surface in a way that the overall antenna characteristics are enhanced [8]. It is clear that in array applications, the effect of mutual coupling is usually undesirable, because it reduces the antenna gain, raises the side lobe level, etc. However, in some applications mutual coupling enhances the antenna performance. For example, in the case of microstrip antenna, parasitic patches can be placed around a driven element to increase the gain of this single driven element by several decibels [9]. Also, it is interesting that parasitic patches with open circuit stubs can shape the beam of antenna so that it is tilted in a desired direction [10].

The first researcher who suggested the use of Yagi-Uda antenna design in microstrip structures was Huang in 1989 [11]. His proposed antenna consisted of four patches that were electromagnetically coupled to each other. That antenna had maximum gain of 8 dBi and low F/B ratio. After that, Huang and Densmor introduced a new microstrip Yagi-Uda antenna that had a maximum gain of 14 dBi but its use in some applications was problematic because of its low F/B ratio. The large size of this antenna was also the source of other difficulties [12]. Later, many methods were proposed to improve the gain and F/B ratio of these antennas, such as using a periodic band-gap (PBG) structure [13]. These periodic structures affect the transmission of propagating waves. Proper utilization of PBGs has potential to improve performances of radiating elements [14–17].

In [18], a new type of microstrip Yagi-Uda antenna was introduced which achieved high gain and high F/B ratio. However, this antenna was single band, working at 5.2 GHz with return loss of 15 dB at this frequency.

In this paper, we present a novel design of broad band microstrip Yagi-Uda antenna which supports 5.2 and 5.8 GHz bands. Our proposed antenna is designed to operate around the 5.5 GHz band, which is used in recent wireless local-area networks (LANs) and is being considered for next-generation mobile communications.

Although the proposed antenna can be scaled to be used at much higher frequencies, such as 34 GHz, this paper discusses only 5.5 GHz band operation since we try to confirm the basic performance of our antenna with little manufacturing error.

The proposed antenna configuration has high gain and high F/B ratio, and the return loss in both bands (5.2 GHz and 5.8 GHz) is more than 20 dB so we can say that our proposed antenna is a very good

candidate for various applications up to the millimeter wave frequency range.

Section 2 briefly reviews the basic idea of our microstrip Yagi-Uda array antenna. Section 3 describes the geometry and operation mechanism of the proposed antenna. In this section, we demonstrate the validity of our proposed design through numerical analyses and experimental results of fabricated antenna. Section 4 discusses parametric analyses of the proposed antenna and clears out the relationship among the parasitic patches. In Section 5, we have combined two of our designed microstrip Yagi-Uda antennas in order to achieve higher gain, and finally the major advantages of this antenna are compared to our primary design of single Yagi-Uda.

Full wave analysis of the proposed antenna configurations were performed using Ansoft HFSS [19] based on finite element method (FEM). In addition, the simulation results were confirmed using CST Microwave Studio [20] which is based on finite integral technique (FIT).

It should be mentioned that, in this paper, by F/B ratio we mean the ratio of front side radiation in the range of $0^\circ \leq \theta \leq 90^\circ$, to the backside radiation in the range of $-90^\circ \leq \theta \leq 0^\circ$.

2. ANTENNA STRUCTURE DESIGN AND SIMULATION

Similar to the classical Yagi-Uda dipole antenna, the microstrip Yagi-Uda antenna consists of a reflector, a driven element and a number of director elements. The reflector element is tuned lower and director elements are tuned higher in frequency than the driven element [6].

Figure 1 shows the microstrip Yagi-Uda antenna that consists of eleven patches with its feeding structure. There are two reflectors (R) and eight directors D_{1_u} (top director 1), D_{2_u} (top director 2), D_{3_u} (top director 3), D_{4_u} (top director 4), and D_{1_L} (bottom director 1), D_{2_L} (bottom director 2), D_{3_L} (bottom director 3), D_{4_L} (bottom director 4)), and also one driven patch (D) that is excited by feeding structure. The feeding structure has a simple construction. It consists of a $50\,\Omega$ feed line that is transformed to high impedance line through the use of a quarter wave transformer. The distance between the elements along the axis is denoted by g (note that these distances are the same). We have also used a high impedance line to reduce the influence of undesirable radiation from the feed. The thickness of the substrate, as shown in Fig. 1, is denoted by h. The antenna is designed on a RT/duriod 5880 ($\varepsilon_r = 2.2$, $\tan\sigma = 0.0009$).

As can be seen in Fig. 1, we have created some slots on 2nd, 3rd and 4th directors. Simulation results show that these slots increase

the mutual coupling between patches and allow us to use more than one director. Actually these patches act as some resonators which are coupled with capacitively gap. These slots change the impedance of these patches in order to improve impedance matching between patches

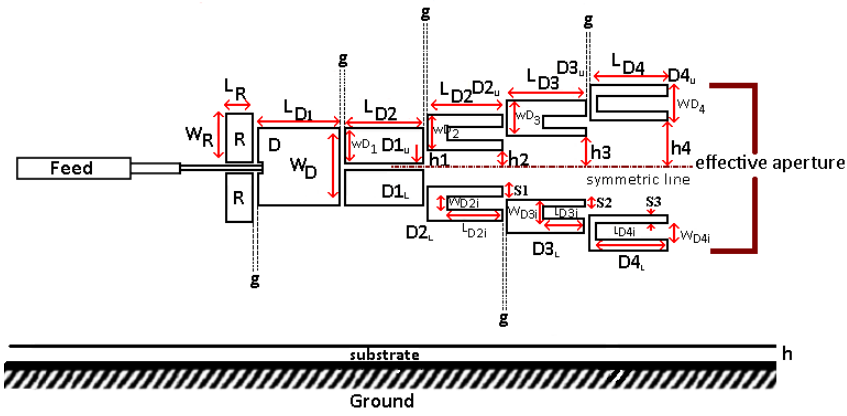

Figure 1. Microstrip Yagi-Uda antenna structure.

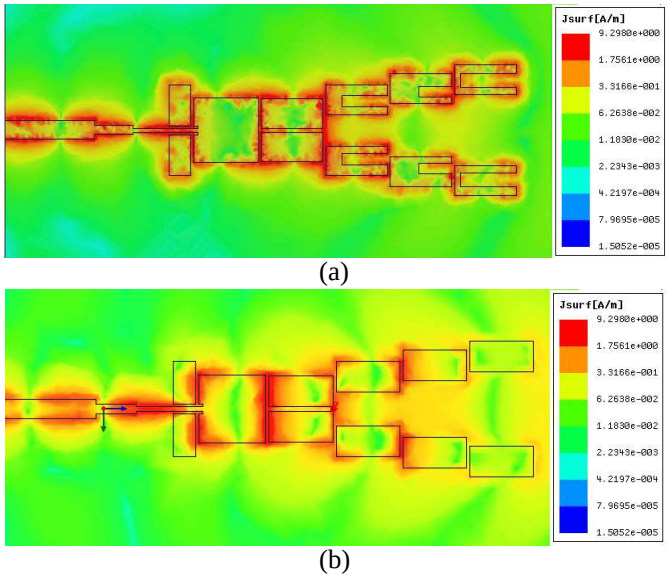

Figure 2. Simulated surface current distributions on the conductors, (a) with slots, (b) without any slots.

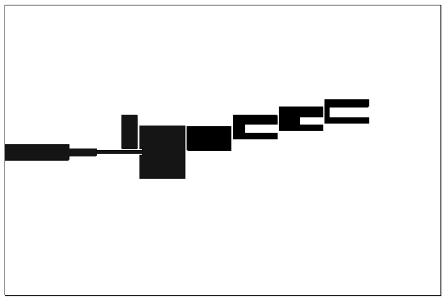

The upper element

(a1)

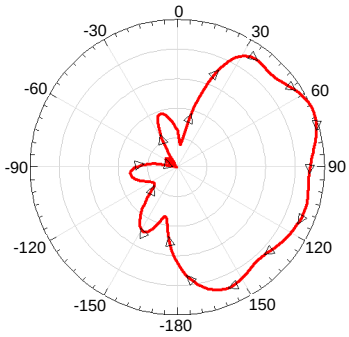

The pattern of upper element

(a2)

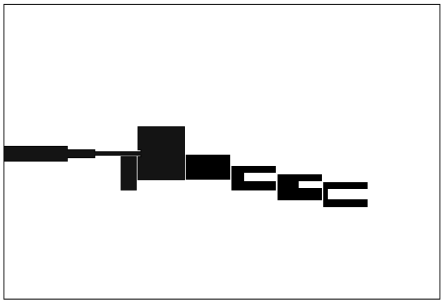

The lower element

(b1)

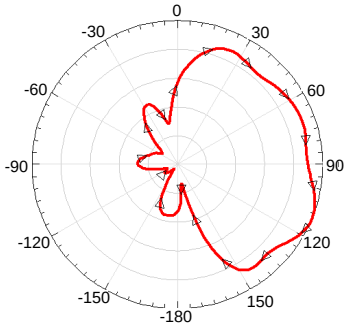

The pattern of lower element

(b2)

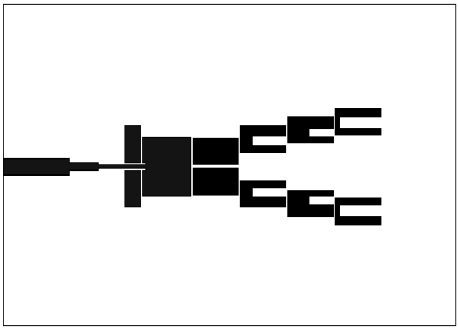

The combined element

(c1)

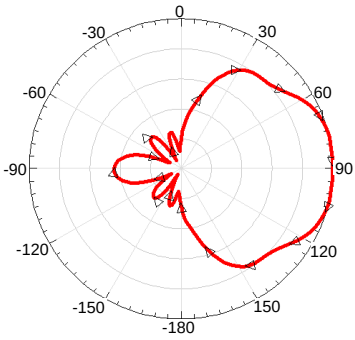

The pattern of the combined element

(c2)

Figure 3. Effect of the upper elements and lower elements.

that lead to better transition of energy from feed point to last patch. Fig. 2 shows the effect of these slots. We have also included a slotless version of our proposed antenna in this figure to provide a better insight of our idea.

From Fig. 2, it is obvious that these slots increase the mutual coupling among the patches, which allows the usage of more patches. However, utilizing 4 additional patches is enough for our application. As can be seen from this figure, the mutual coupling between driven (D) and first director (D_1) is already strong enough that there is no need for the application of any slots on the first director (D_1). The patches have different lengths and thus have different resonance frequencies. The driven element has bigger length and, therefore, has lower resonance frequency. Also, from Fig. 2 we realize that without slots in director patches, the amount of mutual coupling is not sufficient to excite D_2, D_3 and D_4.

We combine the effect of the upper elements (R, D, D_{1_u}, D_{2_u}, D_{3_u}, and D_{4_u}) and the lower elements (R, D, D_{1_L}, D_{2_L}, D_{3_L}, and D_{4_L}) to have a stronger end-fire antenna. Fig. 3 presents the radiation pattern of the upper and lower elements as well as the result of the combined structure. The upper elements have the peak radiation at $60^\circ \leq \varphi \leq 75^\circ$, while the lower elements have the peak radiation at $105^\circ \leq \varphi \leq 120^\circ$. The pattern of the combined element is much stronger at $\varphi = 90^\circ$ (note that the purpose of Fig. 3 is presenting the performance of this antenna, and it will not be utilized in the design process).

In order to increase the gain of the antenna, the distance between upper and lower directors has to be increased [12]. In fact, the intention is increasing the effective aperture of Fig. 1, while the amount of coupling between elements is accounted for. In order to have strong coupling from the driven element D to D_1, we have chosen very small value for h_1. Although, other directors facilitate the presence of more resonance frequencies, these elements also have the role in gain enhancement of the antenna. As the distance between director elements increases, the antenna gain would also increase. However, the inadequate distance enlargement would cause an insufficient coupling between the pervious and newly added patches, so that the gain improvement would be suppressed. The relation among these patches is thoroughly discussed in Section 4.

Note that two reflectors are large enough to decrease the amount of backside radiation. As the simulation results confirm, a larger length is unnecessary for reducing the backside radiation and just causes the antenna gain reduction.

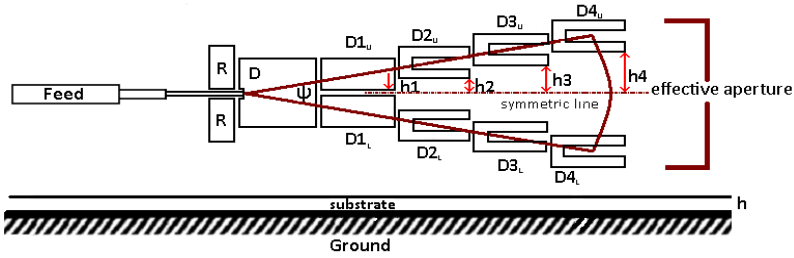

Figure 4. Structure of Microstrip Yagi-Uda antenna with angle of ψ and equal slots.

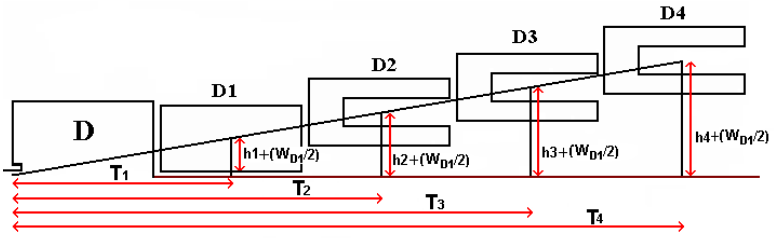

Figure 5. Yagi-Uda's directors that arranged in Thales triangle format.

3. RESULTS AND DISCUSSION

From Fig. 3, it seems that the performance of this antenna is similar to V-dipole antenna. Therefore, we have arranged our antenna in V-shape. Also, in order to simplify the application of GA we arranged directors and driven patches in the Thales triangle format as can be seen in Figs. 4 and 5 and considered equal length and width for all directors.

To achieve the highest gain and front to back ratio, the value of angle ψ in Fig. 4 has to be optimized. In fact, the best value for ψ is equivalent to the best value for h_1, h_2, h_3 and h_4. The following equations can be derived from Fig. 5 to represent the relation between ψ and h_i:

$$T_i = i \times g + [(2i-1)/2] \times L_{D_1} + L_D \quad (1)$$

$$h_i = \tan(\psi/2) T_i - W_{D_1}/2 \quad (2)$$

By optimization of this structure, the best value for ψ is 19.85°.

To provide a proof of concept to cover a band above and below 5.5 GHz for HIPERLAN applications we have simulated our design

using HFSS11 which is a 3-D simulator that solves for the electric and magnetic fields via the finite element method (FEM). To verify the analysis that has been presented for this antenna structure, the design was fabricated and measured, and finally measurement results are compared with the simulation ones. The optimized values for our design to achieve highest gain and F/B ratio and also highest impedance bandwidth are as follows: $L_R = 5.596$, $W_R = 10.353$, $L_D = W_D = 16.739$, $L_{D_1} = L_{D_2} = L_{D_3} = L_{D_4} = 15.934$, $W_{D_1} = W_{D_2} = W_{D_3} = W_{D_4} = 7.812$, $L_{D_{2_i}} = 11.678$, $L_{D_{3_i}} = 8.573$, $L_{D_{4_i}} = 14.462$, $W_{D_{2_i}} = 2.831$, $W_{D_{3i}} = 2.548$, $W_{D_{4_i}} = 3.379$, $S_1 = 1.981$, $S_2 = 1.698$, $S_3 = 1.998$, $h_1 = 0.557$, $h_2 = 3.480$, $h_3 = 6.409$, $h_4 = 9.336$, $g = 0.793$ and The substrate thickness is $h = 1.58$ millimeters.

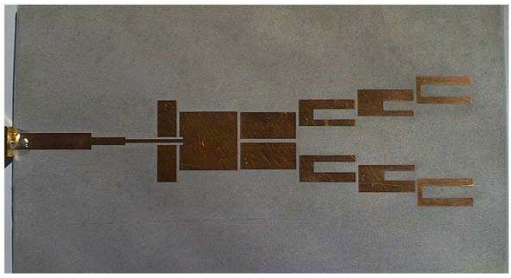

Figure 6. Photograph of our fabricated Microstrip Yagi-Uda antenna.

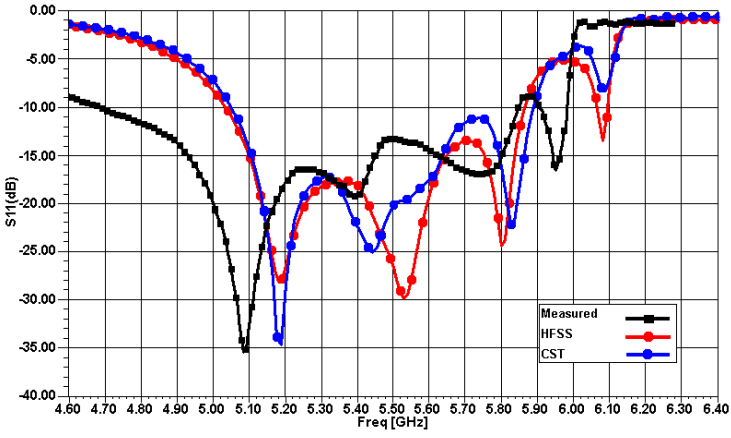

Figure 7. Return loss versus frequency for prototype at a band around 5.5 GHz.

A photograph of this antenna is shown in Fig. 6.

In order to measure the return loss of this antenna, an edge-mount SMA connector was soldered to the edge of the board, and the return loss was measured on a network analyzer. The simulated and measured return loss versus frequency is presented in Fig. 7.

It can be seen that there are more than two resonance frequencies in the plot. The first resonance is due to patch D which is bigger than the other patches. The comparative simulation and measurement results for our proposed antenna are listed in Table 1. The bandwidth of the prototype antenna due to the measurement, 22.05%, is considerably larger than that of the simulated design, 14.87%.

It is clear that the performance of microwave systems is severely affected by tolerances in the fabrication process. There are three frequency shifts in the resonances of the measured design when compared to the simulated results. The third has a frequency shift of 30 MHz which is small for this design. But the frequency shift of 110 MHz at the 5.2 GHz and 5.5 GHz resonance can possibly be attributed to a small tolerance in the substrate (RT/Duroid 5880,

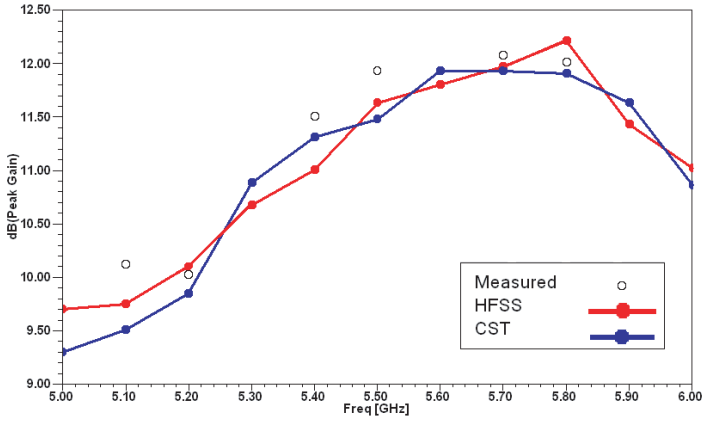

Figure 8. Simulated peak antenna gain against frequency for the proposed antenna.

Table 1.

Yagi structure	HFSS	CST	Measurement
Resonant freq	5.19, 5.60, 5.80	5.18, 5.44, 5.82	5.11, 5.42, 5.78
Bandwidth	5.04–5.85 (14.87%)	5.05–5.90 (15.52%)	4.68–5.84 (22.05%)

$\varepsilon_r = 2.2 \pm 0.02$).

Also the connector was not taken into account in the simulation. The size of the ground plane is 150 mm × 90 mm. Simulation results in Fig. 7 show more than 20 dB of RL in both 5.2 and 5.8 GHz frequencies, which is much better than pervious works [4–12]. The simulated gain of the antenna at different frequencies is given in Fig. 8. The radiation patterns at three frequencies (5.2, 5.5 and 5.8 GHz) are shown in Fig. 9.

It is observed that as the frequency increases, the F/B ratio decreases. At 5.2 GHz, there is no significant backlobe radiation, and the beamwidth is slightly wider. Fig. 10 shows radiation pattern of

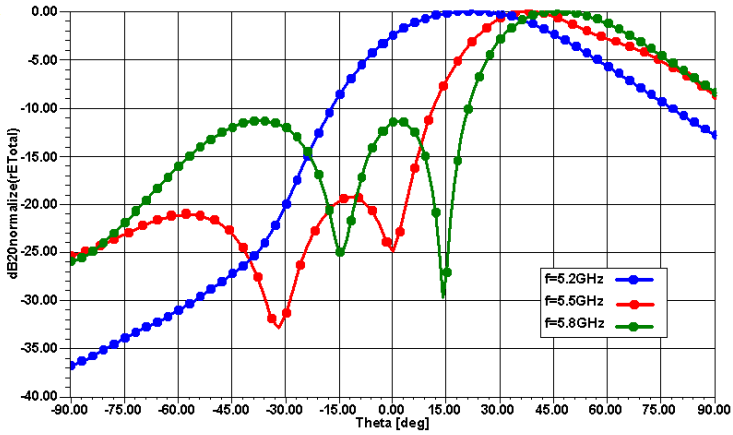

Figure 9. Radiation pattern (Etotal).

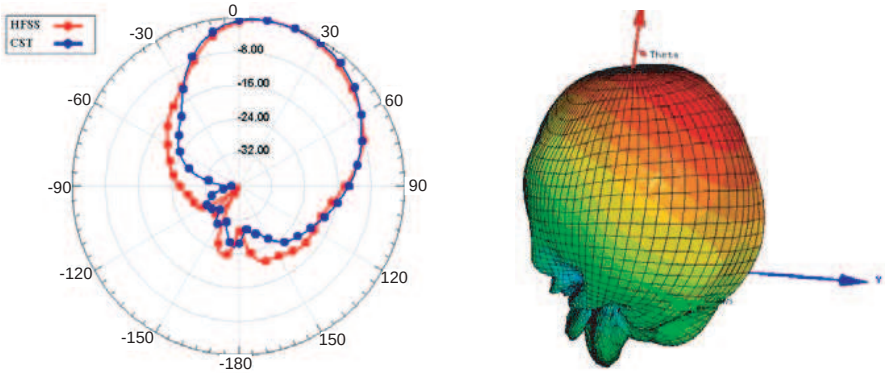

(a) (b)

Figure 10. Radiation pattern (Etotal) at 5.2 GHz, (a) 2D, (b) 3D.

proposed antenna at 5.2 GHz.

The E-plane radiation pattern was measured at 5.5 GHz and compared to the simulated results. This is shown in Fig. 11. The F/B ratio at 5.5 GHz is 18 dB and is much higher than pervious works [4–12].

The patterns of the measured and simulated designs are in good agreement with each other. As can be seen at 5.5 GHz, there exist two backside lobes that are −18 dB and −20 dB down from the main beam. Table 2 shows the comparison of front to back ratio between simulation and measurement results for our proposed antenna at 5.5 GHz.

Gain, F/B ratio and also the beamwidth of these three frequencies (5.2, 5.5 and 5.8 GHz) are shown in Table 3. Note that the results of HFSS and CST are in good agreement.

Table 3 shows the increase of gain due to the increase of frequency so at 5.8 GHz this antenna has best gain but the F/B ratio is less than that of 5.2 and 5.5 GHz.

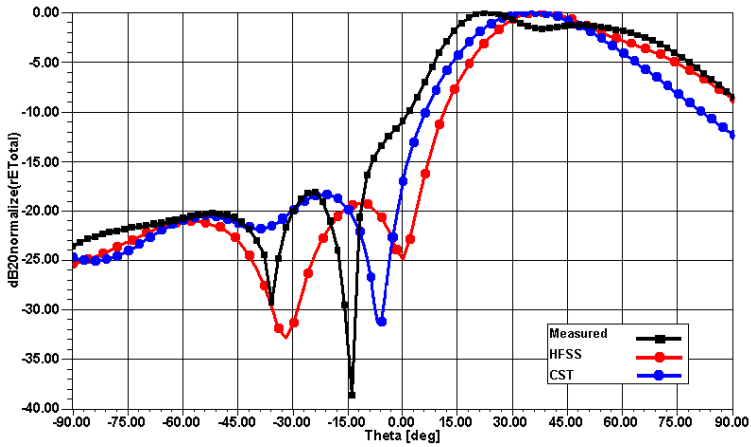

Figure 11. E-plane radiation patterns in rectangular form at 5.5 GHz.

Table 2.

Yagi structure	HFSS	CST	Measured
Front to Back (dB)	19	18.1	18

4. PARAMETRIC ANALYSIS

There are many parameters that need to be addressed in this antenna structure. This section gives insight on how these critical parameters affect the radiation characteristics presented in the tables of this section. The results of various amounts for h_1 are shown on Table 4. Also, instead of studying the effect of h_2, h_3 and h_4 on radiation characteristic of antenna we prefer to study just the effect of ψ which can cover all variation on h_2, h_3 and h_4. These parameters are varied around the optimized values given in the previous section. The results are at 5.5 GHz and show that we have slight variation for the angle of maximum radiation. It should be considered that other parameters are constant and equal to value that achieve in last section.

4.1. Variation of h_1 at 5.5 GHz

As can be seen in Table 4 the increase of h_1 decreases the gain and F/B ratio of the antenna. The major reason for this decline in gain and F/B ratio is the decreased coupling from the driven element to the D_1 element, so we miss an amount of the fields. The best value for this parameter was found to be 0.557 mm.

4.2. Variation of ψ at 5.5 GHz

The variation of ψ is summarized in Table 5. It can be observed that this parameter has a major effect on the gain and F/B ratio because it changes the effective aperture of the antenna. The best value for this parameter was found to be $\psi = 19.85°$.

4.3. Bandwidth Variation

It is evident that only D_1 has a major effect on bandwidth because D_1 is excited more than other directors, so we just study the variations of h_1.

Table 3.

f (GHz)	Gain (dBi)			F/B Ratio (dB)		Beamwidth (degree)	
	Measured	HFSS	CST	HFSS	CST	HFSS	CST
5.2	10.02	10.1	9.85	...	...	54	52
5.5	11.93	11.63	11.48	19	18.1	37	36
5.8	12.01	12.21	11.90	11	10	32	30

Table 4.

h_1 (mm)	Gain (dBi)		F/B (dB)		Angle of max Radiation (deg)	
	HFSS	CST	HFSS	CST	HFSS	CST
0.557	**11.63**	**11.2**	**19**	**17.8**	**37**	**36**
0.855	11	10.9	14	13.6	37	36
1.124	11	11	13	13	37	36
1.368	10.9	10.9	10	8.8	37	36

Table 5.

f	5.2 GHz		5.5 GHz		5.8 GHz	
ψ	Gain (dBi)	F/B (dB)	Gain (dBi)	F/B (dB)	Gain (dBi)	F/B (dB)
12.35	9.4	...	10.44	12	11.9	8
14.70	9.7	...	10.83	13	12	10
17.20	10	...	11.45	15	12	10.5
19.85	**10.1**	...	**11.63**	**19**	**12.21**	**11**
22.85	10.2	23	11.40	16	12	8
26.50	9.9	17	11.02	15	11.3	5
30.15	9.6	14	10.81	11	10	3
34.2	9.6	10	10.32	8	10.7	3
37.5	8.7	9	9.76	5	10.2	2

As the value of h_1 increases, the coupling is reduced to a point where there is no coupling between the driven and D_1 elements. Therefore, the driven element is the only resonant element. This is seen in Fig. 12 at three values of h_1. As h_1 becomes larger, the higher resonance decreases to a point that only the driven patch resonance is present.

5. COMPARISON OF SINGLE YAGI-UDA ANTENNA WITH ITS DOUBLE COUNTER PART

In order to attain the gain enhancement, we proposed the antenna structure of Fig. 13(a). This structure is composed of two of our initial single Yagi-Uda antennas. The gain improvement mechanism is through the constructive interference of two single Yagi-Uda antennas. Fig. 13(b) exhibits the surface current distribution on the conductor which confirms the excitation of all patches, regardless of the increasing

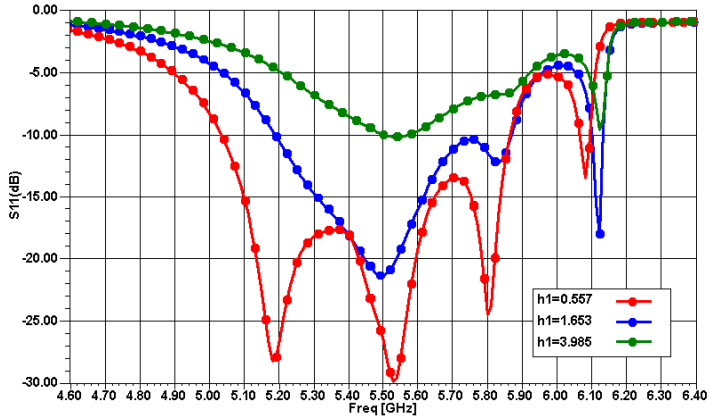

Figure 12. Return loss versus frequency at three values of h_1.

in the number of patches. Note that all dimensions are chosen to be the same as our primary design of single Yagi-Uda antenna with the value of L equal to 30 mm. The simulation results reveal that the better results could be obtained if the inner reflector is removed from each branch. This antenna is designed on a RT/duroid 5880 substrate ($\varepsilon_r = 2.2$, $\tan\sigma = 0.0009$ at 10 GHz) with the operating frequency around 5.5 GHz. The major advantages of this antenna are compared to our primary design of single Yagi-Uda in Figs. 14 and 15.

Figure 14 shows the return loss of double-Yagi-Uda which is compared to primitive single Yagi-Uda antenna. It can be observed that the bandwidth of double-Yagi-Uda antenna, 19.44%, is considerably larger than the bandwidth of single Yagi-Uda antenna,

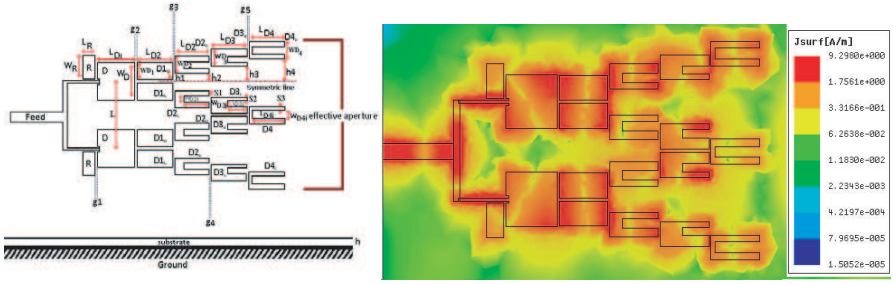

(a) (b)

Figure 13. (a) Double-Yagi-Uda antenna structure, (b) simulated Surface current distributions on the conductors.

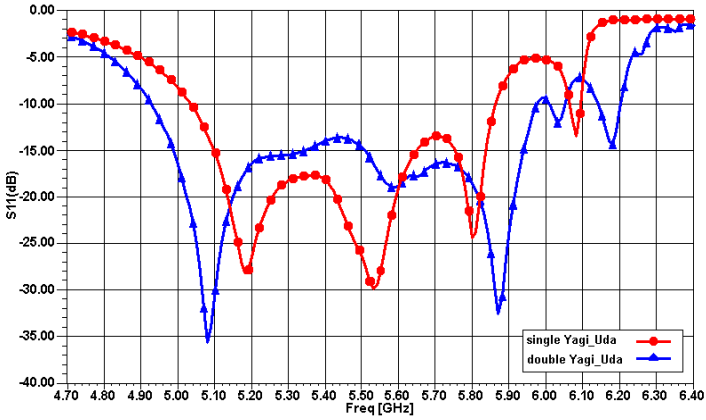

Figure 14. Simulated return loss of double and single Yagi-Uda antenna.

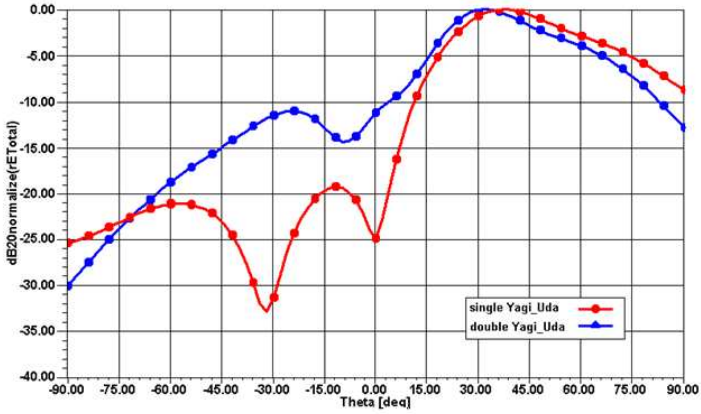

Figure 15. 2-D radiation pattern of the double-Yagi and single-Yagi array at 5.5 GHz.

14.87%.

The radiation pattern of this antenna at 5.5 GHz is illustrated as well as its comparison with the radiation pattern of our initial antenna in Fig. 15.

The angle of maximum radiation for both antennas is between 30°–40°, while the beamwidth is approximately 35°. The gain and front to back ratio for both antennas are presented at three frequencies (5.2, 5.5, 5.8 GHz) in Table 6.

Table 6.

f (GHz)	Gain (dBi)		F/B (dB)	
	double-Yagi	Single Yagi	double-Yagi	Single Yagi
5.2	13.03	10.1	20	...
5.5	14.31	11.63	12	19
5.8	14.82	12.21	8	11

6. CONCLUSION

In this work, a novel Wide-Band Microstrip Yagi-Uda antenna was presented. This antenna has high F/B ratio up to 18 dB and high gain of more than 10 dBi. The antenna is a good candidate for the applications where the backside radiation needs to be suppressed. An impedance bandwidth of 22.05% was obtained which is much higher than previously reported results of other researchers. This antenna covers the frequency band of 5.04–5.85 GHz with minimum value of 13 dB for return loss, thus, being suitable for wide-band application. Also, the antenna presents a minimum 20 dB return loss at 5.2 and 5.8 GHz frequencies, therefore, demonstrating dual band characteristics. This feature makes the proposed antenna appropriate for many applications such as radar and wireless networks, furthermore. It could be easily integrated to ISM (industrial, scientific, and medical) and millimeter wave applications.

REFERENCES

1. Takimoto, Y., "Recent activities on millimeter wave indoor LAN system development in Japan," *Dig. IEEE Microwave Theory and Techniques Society Int. Symp.*, 405–408, Jun. 1995.
2. Morinaga, N. and A. Hashimoto, "Technical trend of multimedia mobile and broadband wireless access systems," *Trans. IEICE*, Vol. E82-B, No. 12, 1897–1905, Dec. 1999.
3. Wu, Y.-J., B.-H. Sun, J.-F. Li, and Q.-Z. Liu, "Tripl-band omni-directional antenna for WLAN application," *Progress In Electromagnetics Research*, PIER 76, 477–484, 2007.
4. Misra, I. S., R. S. Chakrabarty, and B. B. Mangaraj, "Design, analysis and optimization of V-dipole and its three-element Yagi-Uda array," *Progress In Electromagnetics Research*, PIER 66, 137–156, 2006.

5. Tran, A. and M. C. E. Yagoub, "Intertwined two-section dual-polarized log periodic dipole antenna," *PIERS Proceedings*, 30–33, Prague, Czech Republic, Aug. 27–30, 2007.
6. Densmore, A. and J. Huang, "Microstrip Yagi antenna for mobile satellite service," *IEEE Antennas and Propagation Society Int. Symp.*, Vol. 2, 616–619, Jun. 1991.
7. Zhang, X. C., J. G. Liang, and J. W. Xie, "The Quasi-Yagi antenna subarrat fed by an orthogonal T junction," *Progress In Electromagnetics Research Letters*, Vol. 4, 109–112, 2008.
8. Chen, C. A. and D. K Cheng, "Optimum element lengths for Yagi-Uda arrays," *IEEE Trans. Antennas and Propagation*, Vol. 23, Jan. 1975.
9. Lee, K. F., et al., "Microstrip antenna array with parasitic elements," *IEEE Antennas and Propagation Society Symposium Dig.*, 794–797, Jun. 1987.
10. Haneishi, M., et al., "Beam-shaping of microstrip antenna by parasitic elements having coaxial stub," *Trans. IECE of Japan*, Vol. 69-B, 1160–1161, 1986.
11. Huang, J., "Planar microstrip Yagi array antenna," *IEEE Antennas and Propagation Society Int. Symp.*, Vol. 2, 894–897, Jun. 1989.
12. Gray, D., J. Lu, and D. Thiel, "Electronically steerable Yagi-Uda microstrip patch antenna array," *IEEE Trans. Antennas and Propagation*, Vol. 46, No. 5, 605–608, May 1998.
13. Padhi, S. and M. Bialkowski, "Investigations of an aperture coupled microstrip Yagi antenna using PBG structure," *IEEE Antennas and Propagation Society Int. Symp.*, Vol. 3, 752–755, Jun. 2002.
14. Yablonovitch, E., "Photonic band-gap structures," *Journal of Optical Society of America B*, Vol. 10, 283–295, 1993.
15. Yang, F., K. Mu, Y. Quin, and T. Itoh, "A unipolar photonic bandgap (UC-PBG) structure and its applications for microwave circuits," *IEEE Trans. Microwave Theory Technique*, Vol. 47, 1509–1514, Aug. 1999.
16. Fu, Y. Q., G. H. Zhang, and N. C. Yuan, "A novel PBG coplanar waveguide," *IEEE Microwave and Wireless Components Letters*, Vol. 11, Nov. 2001,
17. Gonzalo, R., P. D. Maagt, and M. Sorolla, "Enhanced patch-antenna performance by suppressing surface waves by using photonic bandgap substrates," *IEEE Trans. Microwave Theory and Techniques*, Vol. 47, 2131–2139, Nov. 1999.

18. DeJean, G. R. and M. M. Tentzeris , "A new high-gain microstrip Yagi array antenna with a high front-to-back (F/B) ratio for WLAN and millimeter-wave applications," *IEEE Trans. Antennas and Propagation*, Vol. 55, Feb. 2007.
19. HFSS: High frequency structure simulator based on the finiteElement method, v. 9.2.1, Ansoft Corporation, 2004.
20. CST GmbH 2008 CST MICROWAVE STUDIO(r) User Manual V. 5.0, Darmstadt, Germany (www.cst.de).
21. R/T Duroid Laminates, Rogers Corporation, Rogers, CT, 2008.